

## Empirical Interatomic Potential for Carbon, with Applications to Amorphous Carbon

J. Tersoff

*IBM Research Division, T. J. Watson Research Center, Yorktown Heights, New York 10598*

(Received 10 May 1988)

An empirical interatomic potential is introduced, which gives a convenient and relatively accurate description of the structural properties and energetics of carbon, including elastic properties, phonons, polytypes, and defects and migration barriers in diamond and graphite. The potential is applied to study amorphous carbon formed in three different ways. Two resulting structures are similar to experimental *a*-C, but another more diamondlike form has essentially identical energy. The liquid is also found to have unexpected properties.

PACS numbers: 61.45.+s, 61.40.+b, 61.70.Bv

Carbon holds a special place among the elements. Its uniquely strong bonds and high melting point make it at once fascinating and technologically important. Yet our understanding of condensed phases of carbon is still in its infancy.

The purpose of this paper is twofold. First, an empirical interatomic potential for carbon is introduced, and tested by calculating the energy and structure of numerous polytypes of carbon, and the elastic properties, phonons, defect energies, and migration barriers in diamond and graphite. The accuracy, based on comparison with experiment or with state-of-the-art quantum mechanical calculations<sup>1-4</sup> in the local-density approximation (LDA), is quite impressive given the simplicity of the model potential.

The potential is then applied to study the structural properties of amorphous carbon (*a*-C). The study of disordered phases is extremely challenging both experimentally and theoretically, and limited LDA studies are only beginning to become feasible.<sup>5</sup> Here, samples of *a*-C are computer generated in different ways; by homogeneously condensing the vapor or by quenching the liquid. Both methods lead to a very similar structure, which is consistent with measured properties of *a*-C. However, quenching the liquid under megabar pressure leads to a denser more diamondlike amorphous phase, which has an energy essentially identical to that of the ordinary phase. The structure of the liquid itself is also found to be surprising, with a low density and less than three neighbors per atom on the average.

There are tremendous practical advantages to a classical interatomic potential, where the energy is modeled empirically as an explicit function of atomic coordinates. However, the ability of such a potential to accurately describe the diverse properties of real materials remains controversial. For that reason, a substantial part of this paper is devoted to establishing the accuracy of the present potential in a wide range of conventional applications, before using it to study *a*-C, which is relatively poorly understood.

The ideas upon which the present potential is based were described in two earlier papers<sup>6,7</sup> which treated silicon. The form of the potential used here is identical to that of Ref. 7, but with different numerical values for the parameters. The fact that the same form works well for both silicon and carbon provides further evidence for the generality of this approach.

The parameters in the potential are chosen primarily by fitting the cohesive energies of carbon polytypes, along with the lattice constant and bulk modulus of diamond. Values calculated by Yin and Cohen<sup>1</sup> are used where measurements are not available. However, as an additional constraint, the vacancy in diamond is required to have a formation energy of at least 4 eV, to avoid a large discrepancy with the value of 7 eV found by Bernholc *et al.*<sup>3</sup> (Parameters obtained without this constraint give a vacancy formation energy under 2 eV, but otherwise give results rather similar to those presented here.)

The resulting parameters for carbon are as follows:  $A=1393.6$  eV,  $B=346.74$  eV,  $\lambda_1=3.4879$  Å,  $\lambda_2=2.2119$  Å,  $\beta=1.5724\times 10^{-7}$ ,  $n=0.72751$ ,  $c=38049$ ,  $d=4.3484$ ,  $h=-0.57058$ ,  $R=1.95$  Å, and  $D=0.15$  Å. It should be stressed that, as discussed in Ref. 7,  $R$  and  $D$  were chosen somewhat arbitrarily and were not systematically optimized. For simplicity, the parameters  $a$  and  $\lambda_3$  have been set equal to zero here.

The very short range of the potential (2.1 Å) precludes treating dihedral-angle forces or the weak interlayer forces in graphite, or distinguishing between even and odd numbered rings (which appear to play a role in "magic numbers" of small clusters). However, in view of the tremendous computational advantages of the short range, no attempt was made to incorporate these more subtle effects.

The resulting energies and bond lengths of a number of carbon prototypes are summarized in Fig. 1. The present potential is seen to describe the cohesive energy of carbon quite well over an extreme range of configurations, ranging from the dimer molecule to

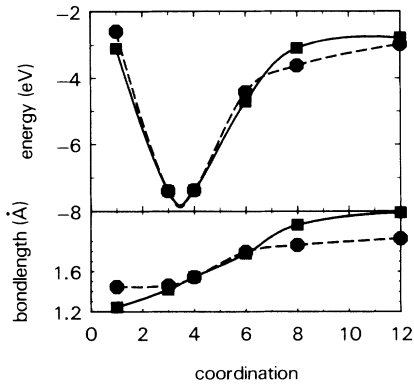


FIG. 1. Cohesive energy per atom (eV), and bond length (Å), plotted vs atomic coordination number, for several real and hypothetical polytypes of carbon:  $C_2$  dimer molecule, graphite, diamond, simple cubic, bcc, and fcc. Squares are experimental values for observed phases, and calculations of Yin and Cohen (Ref. 1) for hypothetical phases. Circles are results of the present model. Lines are spline fits to guide the eye.

close-packed metallic structures. Even the bond-length variations are quite well described for the lower-energy structures.

In addition to describing gross changes in bonding with coordination, it is desirable that such a potential describe small elastic distortions accurately, in order to treat the strain associated with disorder, defects, etc. The calculated elastic moduli and phonon frequencies are summarized and compared with experimental values in Table I. In view of the fact that no energy derivatives other than the diamond bulk modulus were used in determining the parameters, the level of quantitative agreement is impressive.

As an independent test that the role of bond angles is well described, the properties of tetrahedrally coordinated carbon in the BC8 structure are calculated. The energy is found to be 0.6 eV/atom above that of diamond, with the internal structure parameter  $x=0.0967$ , in good agreement with results of Biswas *et al.*<sup>2</sup>

Even the in-plane properties of graphite are adequately described, though the accuracy is less than for dia-

TABLE I. Calculated and measured elastic constants (in Mbar) and phonon frequencies (in THz) of diamond.

Property	Theory	Experiment
$c_{11}$	10.9	10.8
$c_{12}$	1.2	1.3
$c_{44}$	6.4	5.8
LTO( $\Gamma$ )	46.8	39.9
LOA( $X$ )	39.0	35.7
TO( $X$ )	33.6	32.3
TA( $X$ )	24.1	24.0

mond. Here  $c_{11}=12.1$  Mbar (with the crystal fixed at the experimental  $c/a$  ratio), 14% larger than experiment. The shear constant  $c_{66}=(c_{11}-c_{12})/2=7.0$  Mbar, about 40% too high compared with experiment, reflecting excessive bond-angle stiffness. Interlayer forces are of course zero in this short-ranged model.

Energies of point defects are crucial in determining the mechanism and rate of diffusion in solids, and have therefore been widely studied in a range of materials. Such defects represent a particularly stringent test of an empirical potential. Results for a very extensive set of point defects in both diamond and graphite are summarized in Table II. Periodic boundary conditions are used, with cells of 216 atoms. Results of recent LDA calculations<sup>3,4</sup> for relaxed geometries are given for comparison.

In diamond, overcoordinated interstitials, in the tetrahedral or hexagonal hollow sites, are found to have very high energies, roughly 20 eV. Undercoordinated, interstitials, in the split or bond-centered configurations, have lower energies: 10 and 15 eV, respectively. These values are in excellent agreement with recent results of Bernholc *et al.*,<sup>3</sup> except that those authors found a higher energy of 17 eV for the split interstitial. These formation energies are all considerably greater than the cohesive energy (7 eV), in contrast with silicon, where interstitial formation energies are all comparable to the cohesive energy.

To check whether the lowest-energy interstitial configuration has actually been found, simulation of annealing has been performed at 2000 K, starting with the tetrahedral-site interstitial. The split interstitial geometry is obtained, suggesting that this is indeed the

TABLE II. Calculated defect energies in diamond and graphite, in eV, and results of previous LDA calculations (diamond, Ref. 3; graphite, Ref. 4). Here "vac," "int," and "exch" denote vacancy, interstitial, and the assumed saddle point for direct exchange.

Defect	Theory	LDA
Diamond		
vac	4.3	7.2
split vac	9.7	9.0
int( $T$ )	19.6	23.6
int( $H$ )	20.9	...
int( $X$ )	16.6	...
int( $B$ )	14.6	15.8
int( $S$ )	10.0	16.7
exch	10.3	13.2
Graphite		
vac	7.1	7.6
split vac	10.8	9.2
int( $B$ )	20.1	...
int( $H$ )	31.4	19.5
exch	13.3	10.4

optimum interstitial geometry with the present potential.

The migration of interstitials provides one possible mechanism for self-diffusion in diamond. An alternative, the concerted exchange mechanism proposed by Pandey<sup>8</sup> for self-diffusion in silicon, gives a migration barrier in diamond of 10 eV with this potential, considerably less than the 15 eV needed for formation plus migration of an interstitial. This value is again in reasonable agreement with Ref. 3. Finally, formation of vacancies plus migration via the split vacancy costs only 9.7 eV with this potential, in quite good agreement with Ref. 3.

Ideally, the potential should describe defects in graphite, as well as in diamond. While the short range of the potential precludes describing the weak interlayer interaction in graphite, recent interest has focused on in-plane defects.<sup>4</sup> Results for several such defects in graphite are listed in Table II, and compared with recent calculations of Kaxiras and Pandey.<sup>4</sup> The agreement is quite satisfactory, especially with respect to trends. In particular, these results lead to the conclusion that for in-plane diffusion in graphite, vacancy migration has an activation energy (10.8 eV) roughly 2–3 eV lower than that for direct exchange (13.3 eV). This is in contradiction to earlier proposals<sup>9</sup> but in agreement with recent conclusions of Ref. 4.

Having thus established its accuracy in an extremely wide range of applications, the present potential is used to study the structure of amorphous carbon. Typically, *a*-C is made by vapor deposition, but for convenience here it is generated either by homogeneous condensation of a vapor, or by ultrafast quenching of liquid carbon. Samples of 216 atoms with periodic boundary conditions are treated with use of a continuous-space Monte Carlo method.<sup>10</sup> The cell volume is allowed to vary, and a modest pressure of 10 kbar is maintained to prevent the formation of voids and to speed the annealing process.

The condensed-vapor samples begin at about 200 times the diamond volume, and so the atoms must drift randomly for a considerable distance before meeting and forming clusters, which gradually agglomerate. Meanwhile the cell is allowed to slowly shrink under the slight applied pressure. The temperature is maintained at 4000 K for up to 40 000 steps/atom. (The melting temperature for this potential appears to be of order 6000 K, compared to an experimental value of about 4300 K.) The sample is then cooled to 300 K at zero pressure, and its shape is allowed to change freely to relieve strain. The sample with the longest annealing is designated sample 1.

The quenched-liquid samples are cooled from 12 000 to 300 K at inverse rates of up to 8 steps/atom-K. Below 1000 K, the pressure is removed, and the sample shape is allowed to vary. The sample with the slowest quench is designated sample 2.

The properties of the resulting samples are summarized in Table III, and are consistent with what is known<sup>11</sup> about the structure of *a*-C. Samples 1 and 2

TABLE III. Calculated properties of amorphous carbon samples at 300 K: average coordination  $z$ , average near-neighbor bond length  $r_0$ , average energy per atom relative to diamond, and average density relative to diamond.

Sample	$z$	$r_0$ (Å)	$E$ (eV)	$\rho/\rho_{\text{dia}}$
1 (condensed)	3.08	1.47	0.39	0.62
2 (quenched)	3.09	1.47	0.42	0.68
3 (Mbar)	3.40	1.51	0.43	0.86

are almost indistinguishable in their properties, despite the radically different formation processes, suggesting that there exists a fairly well-defined *a*-C structure independent of preparation procedure.

The radial distribution function (RDF) of sample 2 is shown in Fig. 2(a) (solid line); that of sample 1 is very similar. The first-neighbor peak (designated  $r_0$  in Table III) is centered around 1.47 Å, which is much closer to the graphite bond length (1.46 Å for this potential) than to the diamond bond length (1.54 Å). The peak contains about 3.08 neighbors, with most atoms threefold coordinated. The bond-angle distribution (not shown) is sharply peaked around the graphite bond angle of 120°. Thus, at least locally, the structure looks rather graphitic, in agreement with experiment.<sup>11</sup>

The density of the *a*-C formed here is about 0.65 of the density of diamond. Experimentally, the density of *a*-C is believed<sup>11</sup> to be somewhat lower, 0.40 to 0.60 of the diamond density, but this modest difference may be attributable simply to the absence of voids in such a small sample, and in particular to the fact that the sam-

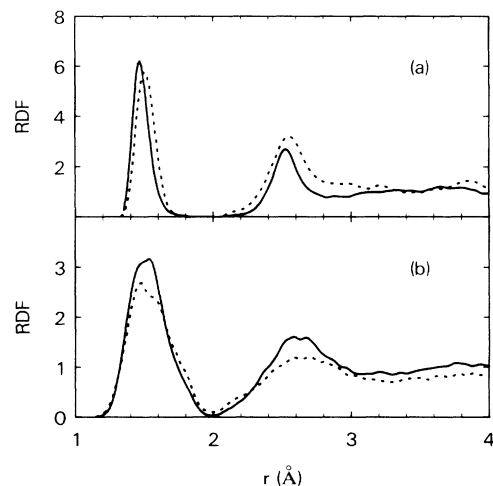


FIG. 2. Calculated radial distribution functions (RDF) of amorphous and liquid carbon, with arbitrary normalization. (a) RDF for sample 2 (solid line), ordinary *a*-C, and for sample 3 (dotted line), *a*-C formed at 1-Mbar pressure. (b) RDF for liquid carbon at 6000 K (solid line) and 8000 K (dotted line).

ple was formed under pressure.

It is believed<sup>11</sup> that between 1% and 10% of the atoms in *a*-C are fourfold coordinated. This is consistent with the fact that samples 1 and 2 both have about 9% of the atoms fourfold coordinated, although that number might change with further annealing or with the elimination of any pressure during formation. In both processes some twofold coordinated atoms occur, with formation energies of about 2 eV, but these tend to disappear during annealing.

It is much harder to evaluate whether the medium-range order, for example the ring statistics, are consistent with real *a*-C, since these are difficult to measure experimentally. The absence of any dihedral-angle forces or long-range van der Waals-like forces in the potential could easily distort the medium-range order, leading to larger deviations from graphitic structure than in real *a*-C.

Much of the current interest in carbon is centered on hard diamondlike coatings, which require hydrogenation. To obtain a model for a more diamondlike *a*-C without hydrogenation, molten carbon was quenched under 1 Mbar of pressure, but otherwise as above, and subsequently annealed at 2000 K. The resulting properties are summarized as sample 3 in Table III, and in Fig. 2(a) (dotted line). Here the first-neighbor peak in the RDF is centered around 1.51 Å, closer to the diamond bond length, but is a bit broader than before. It contains 3.40 nearest neighbors, with almost half the atoms being fourfold coordinated. The density is only 14% lower than diamond. The bond-angle distribution (not shown) is broad, somewhat suggestive of two overlapping peaks centered at the diamond and graphitic bond angles (110° and 120°, respectively).

The energies of the three samples are nearly identical, 0.4 eV/atom relative to diamond. It is thus reasonable to infer that both amorphous structures are stable for practical purposes. Under proper conditions, it might be possible to grow the dense phase without applied pressure, in analogy to the growth of diamond films.

Finally, the liquid phase is examined, and is found to have quite unexpected properties. The static tests cannot guarantee that the liquid will be accurately described here. However, a closely related potential for silicon<sup>12</sup> gave a rather good description of the liquid, and so it is expected that the present potential will at least give a *qualitatively* correct description of liquid carbon.

The liquid-carbon RDF at 6000 and 8000 K is shown in Fig. 2(b). As for silicon,<sup>12</sup> the melting point is too high here (perhaps roughly 6000 K compared to about 4300 K experimentally), and the dip in the RDF is exaggerated at the distance at which the potential cuts off (around 2 Å).

The liquid density is predicted to be less than even the amorphous phase, going from 0.5 to 0.4 of the diamond density in the temperature range 6000–8000 K, with the number of neighbors within 2 Å decreasing from 2.8 to 2.4. This is in marked contrast to the density increase and increased coordination found in liquid silicon.

In conclusion, this very simple empirical approach gives a remarkably accurate description of the structural and energetic properties of carbon. The method is able to describe the entire range of polytypes, while at the same time achieving high accuracy in describing the detailed properties of diamond, ranging from small elastic distortions to severely rebonded point defects. Detailed properties of graphite and *a*-C also appear to be given reasonably well, although in those cases few firm results are available for comparison.

It is a pleasure to thank Jerry Bernholc and Efthimios Kaxiras for making their results available prior to publication. Discussions with Giulia Galli and Sokrates Pantelides are gratefully acknowledged, as is the help of Pantelis Kelires and Michael Sabochick in setting up the Monte Carlo simulations, and of Rana Biswas in setting up the BC8 structure. This work was supported in part by ONR Contract No. N00014-84-C-0396.

<sup>1</sup>M. T. Yin and M. L. Cohen, Phys. Rev. Lett. **50**, 2006 (1983), and Phys. Rev. B **29**, 6996 (1984).

<sup>2</sup>R. Biswas, R. M. Martin, R. J. Needs, and O. H. Nielsen, Phys. Rev. B **35**, 9559 (1987).

<sup>3</sup>J. Bernholc, A. Antonelli, T. M. Del Sole, Y. Bar-Yam, and S. T. Pantelides, Phys. Rev. Lett. **61**, 2689 (1988). Geometry and notation for interstitials is given by M. Lannoo and J. Bourgoin, *Point Defects in Semiconductors* (Springer-Verlag, New York, 1983).

<sup>4</sup>E. Kaxiras and K. C. Pandey, Phys. Rev. Lett. **61**, 2693 (1988).

<sup>5</sup>G. Galli, R. M. Martin, R. Car, and M. Parrinello, unpublished, and Bull. Am. Phys. Soc. **33**, 438 (1988).

<sup>6</sup>J. Tersoff, Phys. Rev. Lett. **56**, 632 (1986). A pathology of this potential was pointed out by B. W. Dodson, Phys. Rev. B **35**, 2795 (1987), and corrected in Ref. 7.

<sup>7</sup>J. Tersoff, Phys. Rev. B **37**, 6991 (1988). See also Ref. 12.

<sup>8</sup>K. C. Pandey, Phys. Rev. Lett. **57**, 2287 (1986).

<sup>9</sup>G. J. Dienes, J. Appl. Phys. **23**, 1194 (1952); see also references in G. J. Dienes and D. O. Welch, Phys. Rev. Lett. **59**, 843 (1987).

<sup>10</sup>P. C. Kelires and J. Tersoff, Phys. Rev. Lett. **61**, 562 (1988).

<sup>11</sup>J. Robertson, Adv. Phys. **35**, 317 (1986).

<sup>12</sup>An alternative set of parameters for the potential of Ref. 7, giving improvements in many properties for silicon, is presented in J. Tersoff, Phys. Rev. B (to be published).